Vehicle System Dynamics
International Journal of Vehicle Mechanics and Mobility

ISSN: 0042-3114 (Print) 1744-5159 (Online) Journal homepage: http://www.tandfonline.com/loi/nvsd20

# Hunting stability analysis of high-speed train bogie under the frame lateral vibration active control

Yuan Yao, Guosong Wu, Yousef Sardahi & Jian-Qiao Sun

VEHICLE SYSTEM DYNAMICS, 2018
VOL. 56, NO. 2, 297–318
https://doi.org/10.1080/00423114.2017.1375128



# Hunting stability analysis of high-speed train bogie under the frame lateral vibration active control

Yuan Yao[a], Guosong Wu[a], Yousef Sardahi[b] and Jian-Qiao Sun[b]

[a]Traction Power State Key Laboratory, Southwest JiaoTong University, Chengdu, People's Republic of China; [b]School of Engineering, University of California, Merced, CA, USA

**ABSTRACT**

In this paper, we study a multi-objective optimal design of three different frame vibration control configurations and compare their performances in improving the lateral stability of a high-speed train bogie. The existence of the time-delay in the control system and its impact on the bogie hunting stability are also investigated. The continuous time approximation method is used to approximate the time-delay system dynamics and then the root locus curves of the system before and after applying control are depicted. The analysis results show that the three control cases could improve the bogie hunting stability effectively. But the root locus of low- frequency hunting mode of bogie which determinates the system critical speed is different, thus affecting the system stability with the increasing of speed. Based on the stability analysis at different bogie dynamics parameters, the robustness of the control case (1) is the strongest. However, the case (2) is more suitable for the dynamic performance requirements of bogie. For the case (1), the time-delay over 10 ms may lead to instability of the control system which will affect the bogie hunting stability seriously. For the case (2) and (3), the increasing time-delay reduces the hunting stability gradually over the high-speed range. At a certain speed, such as 200 km/h, an appropriate time-delay is favourable to the bogie hunting stability. The mechanism is proposed according to the root locus analysis of time-delay system. At last, the nonlinear bifurcation characteristics of the bogie control system are studied by the numerical integration methods to verify the effects of these active control configurations and the delay on the bogie hunting stability.

**ARTICLE HISTORY**
Received 15 November 2016
Revised 18 June 2017
Accepted 11 August 2017

**KEYWORDS**
High-speed bogie; hunting stability; active control; time-delay; multi-objective optimisation; finite dimensional state space approximation

## 1. Introduction

Recently, active controls of railway vehicles have been receiving much attention. Most of today's researchers concern with railway vehicle ride comfort, the tilting train control and the secondary suspension semi-active or active control in order to enhance the vehicle lateral and vertical smoothness, and to reduce high-frequency elastic vibration of the car body [1,2]. Since the effect of bogie primary suspension on the critical velocity of railway vehicles

CONTACT Jian-Qiao Sun jqsun@ucmerced.edu

has been well studied, scholars have proposed the use of semi-active and full-active suspension control to improve the lateral stability of the train [3–11]. Many different approaches for active primary suspensions have been reported in the literature [8]. Feedback control of bogie active stability can be applied either directly or indirectly [12]. The direct control involves the application of an actuator onto a solid wheelset or onto an axle with independently rotating wheels. A practical compromise is to apply a yaw torque indirectly at the secondary suspension level, a concept called 'Secondary Yaw Control' . The actuators may be designed to replace the traditional passive yaw dampers so that active control of the running gear can be introduced without a substantial redesign of the bogie, although this means that radical simplifications of the vehicle design may be limited [13].

In the active control design for trains, the lateral hunting stability of railway vehicle at high speed is one of the most concerned dynamic problems especially for high-speed EMU, in which the conflict between the hunting stability and the curving performance is inconspicuous [14]. When the vehicle runs on poor tracks or operating environment, the suspension performances may change during service due to the tread wear and component failure. Loss of the lateral stability causes poor ride comfort or even derail accidents. Active controls in high-speed trains are great alternatives of passive methods because of their flexibility. There are a lot of literature on using active control onto the solid wheelset or independently rotating wheel to improve the stability of the bogie or wheelset, meanwhile, the control scheme also improve the curving performance [15–17]. However, the application of active control onto wheelset directly to improve the running stability still has many challenges in practice.

In this paper, we present an indirect method for improving the bogie hunting stability through controlling the frame lateral vibration. This control method is practicable and riskless in practical application. Three different frame vibration control configurations are proposed and the corresponding bogie dynamics performances are compared. The bogie is not a completely controllable and observable system, a partial subsystem composed of the frame and motors is chosen as the control model to achieve the vibration control. The vibration states of frame and motor need be detected rather than the wheelset. To consider the inherited confliction between the system relative stability and control energy, a multi-objective optimisation is used in the control design. Also, the linear and nonlinear stability of the bogie control system at different running speeds for each control configuration is investigated. Furthermore, the effects of time-delay in control system on the bogie system performances are discussed.



## 2. The frame lateral vibration active control

We consider a simplified model of this system as shown in Figure 1. The model describes the lateral movements of a bogie. We assume that the lateral position of the car body is pre-determined. The bogie frame is assumed to be connected with the fixed coordinate system through the secondary suspension, such as stiffness and damping in the longitudinal and lateral directions. The bogie has two solid axle wheelsets which are attached to the bogie frame via suspension springs in the longitudinal and lateral directions. In fact, due to the gear transmission box or other devices amounted onto the axle, the non-coincidence between the wheelset's mass centre and geometric centre are ignored in this simplified model for the theoretical analysis.

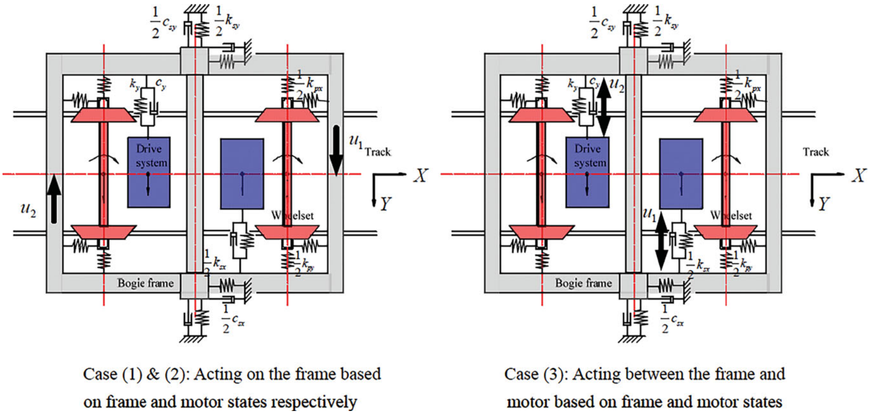


**Figure 1.** Dynamics model of the bogie with three control cases.



The motor or driving system in some high-speed train bogies is connected flexibly to improve the railway vehicle hunting stability at high speed [18]. It means that the motor can move in lateral or yaw direction relative to the frame. The motor is connected to the frame by the elastic and damping elements. The frame and the wheelset in the model have lateral and yaw degrees of freedom, and the motor has only lateral degree of freedom. The dynamic model was found to have 5 rigid bodies and 8 degrees of freedom. The model describes the lateral movements of the bogie and reads,

$$\mathbf{M}\ddot{\mathbf{x}} + \mathbf{C}\dot{\mathbf{x}} + \mathbf{K}\mathbf{x} = \mathbf{Q} + \mathbf{E}\mathbf{u}, \tag{1}$$

where $\mathbf{x} = [y_{w1}, \varphi_{w1}, y_{w2}, \varphi_{w2}, y_f, \varphi_f, y_{m1}, y_{m2}]$. The states $y_{w1}, y_{w2}, y_f, y_{m1}$, and $y_{m2}$ are the lateral displacements of wheelset 1, wheelset 2, frame, motor 1 and motor 2, respectively. While, $\varphi_{w1}$, $\varphi_{w2}$, and $\varphi_f$ represent the yaw angles of wheelset 1, wheelset 2, and frame. The matrices **M**, **C**, and **K**, are the mass, damping and stiffness components of the system. The matrix **Q** is the external force vector, such as the wheel–rail forces caused by the track irregularity and the centrifugal force in curve. In this study, we focus on the bogie linear system and its stability, so the **Q** is a zero vector. The symbols $u_1$ and $u_2$ are the lateral forces applied on the frame or between the frame and motor. The **E** is their vector describing the influence of the control on the system dynamics. These matrices and vectors are listed in the appendix and the values and definitions of system parameters are listed in Table 1. In order to highlight the effect of active control on improving the bogie hunting stability, the damping of yaw damper is one fourth of design value and the analysis of bogie fault state is conducted.

The state equation of the bogie control system can be written as

$$\begin{aligned} \dot{\mathbf{x}}(t) &= \mathbf{A}\mathbf{x}(t) + \mathbf{B}\mathbf{u}(t) + \mathbf{F}\mathbf{d}(t), \\ \mathbf{y} &= \mathbf{D}\mathbf{x}(t), \end{aligned} \tag{2}$$

where $\mathbf{d}(t)$ is the external disturbance such as track irregularity applied on the wheelsets. The state vector is defined as

$$\mathbf{x} = [y_{w_1}, \varphi_{w_1}, y_{w_2}, \varphi_{w_2}, y_f, \varphi_f, y_{m_1}, y_{m_2}, \dot{y}_{w_1}, \dot{\varphi}_{w_1}, \dot{y}_{w_2}, \dot{\varphi}_{w_2}, \dot{y}_f, \dot{\varphi}_f, \dot{y}_{m_1}, \dot{y}_{m_2}]^{\mathrm{T}}. \tag{3}$$

**Table 1.** The bogie model parameters.

| Symbol | Definition | Value |
|---|---|---|
| $m_w$ | Mass of the wheelset | 1639 kg |
| $I_w$ | Yaw inertia of the wheelset yaw inertia | 822 kg m$^2$ |
| $m_f$ | Mass of bogie frame | 2328 kg |
| $I_f$ | Yaw inertia of bogie frame | 4080 kg m$^2$ |
| $m_m$ | Mass of motor | 850 kg |
| $\lambda_e$ | Wheel–rail contact conicity | 0.2 |
| $k_{px}$ | Primary longitudinal stiffness per axle | 60 kN/mm |
| $k_{py}$ | Primary lateral stiffness per axle | 10 kN/mm |
| $k_{sx}$ | Secondary longitudinal stiffness | 0.26 kN/mm |
| $k_{sy}$ | Secondary lateral stiffness | 0.26 kN/mm |
| $c_{sx}$ | Yaw damper damping (fault/design value) | 660/2500 N s/m |
| $c_{sy}$ | Secondary lateral damper damping | 30 kN s/m |
| $2l_1$ | Lateral spacing of primary suspension | 2000 mm |
| $l_e$ | Longitudinal distance from end beam | 1500 mm |
| $2b$ | Wheel base | 2.5 m |
| $2l_0$ | Distance of the contact spot | 1493 mm |
| $2l_2$ | Lateral spacing of the secondary suspension | 2200 mm |
| $l_m$ | Longitudinal distance from motor suspension to bogie centre | 750 mm |
| $r_0$ | The wheel rolling radius | 0.46 m |
| $f_\xi$ | The longitudinal creep coefficient | 1e7 N |
| $f_\eta$ | The lateral creep coefficient | 1e7 N |
| $f_{my}$ | Motor suspension frequency | 3 Hz |
| $\xi_{my}$ | Motor suspension damping ratio (Uncontrol/Control) | 0.2/0.5 |
| $k_{gy}$ | The gravitational stiffness | – |
| $k_{g\psi}$ | The gravitational angular stiffness | – |
| $k_r$ | The contact stiffness of the wheel–rail | 500 kN/mm |
| $v$ | Speed | 350 km/h |

The system matrices **A**, and **B** and the vector **F** are given by,

$$\mathbf{A} = \begin{bmatrix} 0_{8\times 8} & \mathbf{I}_{8\times 8} \\ -\mathbf{M}^{-1}\mathbf{K} & -\mathbf{M}^{-1}\mathbf{C} \end{bmatrix}, \quad \mathbf{B} = \begin{bmatrix} 0_{8\times 2} \\ \mathbf{M}^{-1}\mathbf{E} \end{bmatrix}, \quad F = \begin{bmatrix} 0_{8\times 1} \\ \mathbf{M}^{-1}\mathbf{W} \end{bmatrix}, \tag{4}$$

where the vector **W** is defined as

$$\mathbf{W} = [k_{py}, 0, k_{py}, 0, 0, 0, 0, 0]^{\mathrm{T}}. \tag{5}$$

The active forces exert on the frame or motor to control the movement of wheelset indirectly in this study. It can be shown that the whole system is not completely controllable and observable. In order to control the frame vibration completely, we consider a partial state feedback control applied onto a subsystem, which is consisted of a frame and two motors. The bogie primary and secondary suspension loads can be regarded as external interference to the subsystem. The subsystem has eight state variables. We re-arrange the order of state variables in Equation (3) as follows,

$$\mathbf{x}_N = [y_f, \varphi_f, y_{m_1}, y_{m_2}, \dot{y}_f, \dot{\varphi}_f, \dot{y}_{m_1}, \dot{y}_{m_2}, y_{w_1}, \varphi_{w_1}, y_{w_2}, \varphi_{w_2}, \dot{y}_{w_1}, \dot{\varphi}_{w_1}, \dot{y}_{w_2}, \dot{\varphi}_{w_2}]^{\mathrm{T}}. \tag{6}$$

Let **T** be a matrix that transforms the state vector **x** into the new one, such that $\mathbf{x}_N(t) = \mathbf{T}\mathbf{x}(t)$. The matrices and vectors of the transformed system are given by

$$\mathbf{A}_N = \mathbf{TAT}^{-1}, \quad \mathbf{B}_N = \mathbf{TB}, \mathbf{F}_N = \mathbf{TF}. \tag{7}$$

The transformed state equation of the system reads

$$\begin{bmatrix}\dot{\mathbf{x}}_{N_{8\times1}}(t)\\ \dot{\mathbf{x}}_{N_{8\times1}}(t)\end{bmatrix}=\begin{bmatrix}\mathbf{A}_{N_{8\times8}} & \mathbf{A}_{N_{8\times8}}\\ \mathbf{A}_{N_{8\times8}} & \mathbf{A}_{N_{8\times8}}\end{bmatrix}\begin{bmatrix}\mathbf{x}_{N_{8\times1}}(t)\\ \mathbf{x}_{N_{8\times1}}(t)\end{bmatrix}+\begin{bmatrix}\mathbf{B}_{N_{8\times2}}\\ 0_{8\times2}\end{bmatrix}\mathbf{u}(t)+\begin{bmatrix}0_{8\times1}\\ \mathbf{F}_{N_{8\times1}}\end{bmatrix}\mathbf{d}(t), \quad (8)$$

The first eight states are belong to the subsystem, which is defined by the following state equations:

$$\dot{\mathbf{x}}_{N_{8\times1}}=\mathbf{A}_{N_{8\times8}}\mathbf{x}_{N_{8\times1}}(t)+\mathbf{A}_{N_{8\times8}}\mathbf{x}_{N_{8\times1}}(t)+\mathbf{B}_{N_{8\times2}}\mathbf{u}(t). \quad (9)$$

The subsystem is completely controllable in the proposed three cases, while the second term $\mathbf{A}_{N_{8\times8}}\mathbf{x}_{N_{8\times1}}(t)$ acts as a disturbance to this subsystem.

We consider a partial state linear feedback control $\mathbf{u}=-\mathbf{K}_c\cdot\mathbf{x}_c(t)$. Where, $\mathbf{K}_c$ is the feedback gain matrix and $\mathbf{x}_c$ is the partial feedback states. In this study, the wheelset hunting is controlled indirectly by controlling the frame lateral vibration. To this end, we consider three different control configurations as shown in Figure 1. The actuator arrangement in case (1) & (2) is that the active control forces exert on the front and rear end beam of frame by two inertial actuators. For some high-speed bogies in which the motors are suspended flexibly in lateral direction, we can install a retractable actuator between the motor and the side beam of frame to achieve the frame vibration control as shown in case (3). In the three cases, the bogie dynamics parameters are exactly the same.

Where, $\mathbf{x}_c$ is shown as following,

$$\mathbf{x}_c=\begin{cases}[y_f,\varphi_f,\dot{y}_f,\dot{\varphi}_f] & \text{for case}(1)\\ [y_{m_1},y_{m_2},\dot{y}_{m_1},\dot{y}_{m_2}] & \text{for case}(2)\\ [y_f,\varphi_f,y_{m_1},y_{m_2},\dot{y}_f,\dot{\varphi}_f,\dot{y}_{m_1},\dot{y}_{m_2}] & \text{for case}(3)\end{cases}. \quad (10)$$

Using this control law, the closed-loop dynamic matrix of the system reads

$$\mathbf{A}_{cl}=\mathbf{A}_N-\mathbf{B}_N[\mathbf{K}_c \quad 0]. \quad (11)$$

We have found that when a control gain $\mathbf{K}_c$ is selected to stabilise the subsystem (9), the overall closed-loop system $\mathbf{A}_{cl}$ is also stable. Nevertheless, stability of the closed-loop system puts a constraint on the control design. In addition to the stability of the closed-loop system, the stability margin and energy efficiency of the controller should be also taken into account in the design. These requirements will be set up and defined in Section 3.

## 3. The multi-objective optimal control

### 3.1. Multi-objective optimisation

A multi-objective optimal control (MOOP) can be stated as follows:

$$\min_{\mathbf{k}\in Q}\{\mathbf{F}(\mathbf{k})\}, \quad (12)$$

where $\mathbf{F}$ is the map that consists of the objective functions $f_i : Q\rightarrow R^1$ under consideration.

$$\mathbf{F}: Q\rightarrow\mathbf{R}^k, \quad \mathbf{F}(\mathbf{k})=[f_1(\mathbf{k}),\ldots,f_k(\mathbf{k})]. \quad (13)$$

$\mathbf{k} \in Q$ is a $q$-dimensional vector of design parameters. The domain $Q \subset \mathbf{R}^q$ can in general be expressed by inequality and equality constraints:

$$Q = \{\mathbf{k} \in \mathbf{R}^q \,|\, g_i(\mathbf{k}) \leq 0, \quad i = 1, \ldots, l, \text{ and } h_j(\mathbf{k}) = 0, \ j = 1, \ldots, m\}. \tag{14}$$

The concept of *dominancy* [19] defined below plays an important role in defining the optimal solution of the MOOP.

**Definition 3.1:** (a) Let $\mathbf{v}, \mathbf{w} \in \mathbf{R}^k$. The vector $\mathbf{v}$ is said to be *less than* $\mathbf{w}$ (in short: $\mathbf{v} <_p \mathbf{w}$), if $v_i < w_i$ for all $i \in \{1, \ldots, k\}$. The relation $\leq_p$ is defined analogously.
(b) A vector $\mathbf{v} \in Q$ is called *dominated* by a vector $\mathbf{w} \in Q$ ($\mathbf{w} \prec \mathbf{v}$) with respect to the MOOP (12) if $\mathbf{F}(\mathbf{w}) \leq_p \mathbf{F}(\mathbf{v})$ and $\mathbf{F}(\mathbf{w}) \neq \mathbf{F}(\mathbf{v})$, else $\mathbf{v}$ is called non-dominated by $\mathbf{w}$.

If a vector $\mathbf{w}$ dominates another vector $\mathbf{v}$, then $\mathbf{w}$ can be considered to be a 'better' solution of the MOOP. The definition of optimality or the 'best' solution of the MOOP is now straightforward.

**Definition 3.2:** (a) A point $\mathbf{w} \in Q$ is called *Pareto optimal* or a *Pareto point* of MOOP (12) if there is no $\mathbf{v} \in Q$ which dominates $\mathbf{w}$.
(b) The set of all Pareto optimal solutions is called the *Pareto set* denoted as

$$\mathcal{P} := \{\mathbf{w} \in Q : \mathbf{w} \ \text{ is a Pareto point of MOOP (12)}\}. \tag{15}$$

(c) The image $\mathbf{F}(\mathcal{P})$ of $\mathcal{P}$ is called the *Pareto front*.

The Pareto set and Pareto front typically form $(k-1)$-dimensional manifolds under certain mild assumptions on the MOOP. Recent studies seem to suggest that the Pareto front may have fine structures for MOOPs of complex dynamical systems [20]. Some of the methods used to solve the MOOPs have been discussed in Refs. [21,22]. In this paper, we used the non-dominated sorting genetic algorithm (NSGA-II).

### 3.2. NSGA-II

NSGA developed in [23] is a non-domination based genetic algorithm. Even though it performs well in solving MOOPs, its high computation effort, lack of elitism and implementation of what is called the sharing parameter necessitate improvements. As a result, a modified version of the algorithm named NSGA-II was presented in [24]. The new version has a better sorting algorithm, includes elitism, eliminates the need for the sharing parameter and has less computational burden.

The algorithm incorporates five basic stages [24]. It starts with the initialisation process in which a random population that satisfies the constraints on the design parameters is generated. Once the population is initialised, the sorting stage takes place. In this stage, the candidate solutions are sorted based on their non-domination and placed into different fronts. The solutions in the first front dominate all the other individuals while those in the second front are dominated only by the members in the first front. Similarly, the solutions in the third front are dominated by individuals in both the first and second fronts, and so on. Each candidate solution is given a rank number of the front where it resides.

For instance, members in first front are ranked 1 and those in second are given a rank of 2 and so on. To improve the diversity of the solution, a parameter called the crowding distance is computed for each solution in the third stage. This parameter measures how close an individual is to its neighbours. The larger the average crowding distance, the better the diversity of the population. In the fourth stage, the parents for the next generation are selected. The binary tournament selection method is used for this purpose. A candidate solution is selected if its rank is smaller than the other or if its diversity measure is bigger than the other. In the fifth stage, the simulated binary crossover [25,26] and polynomial mutation [27] operators are applied to produce new children. In the last stage, the new children is merged with the current population. This combination guarantees the elitism of the best individuals. After that, the population is now sorted based on non-domination. The new generation is produced from each front subsequently until the population size goes beyond the current population size. If by adding all the members in front $J$, the population size becomes larger than the current population size, then the individuals in this front are selected based on their crowding distance in the descending order until the population size reaches $N$. The process repeats to generate subsequent generations.

### 3.3. Multi-objective optimal control design

We consider the MOOP design with the gain $\mathbf{K}_c = [k_1, \ldots, k_n]$ as design parameters for the system discussed in Section 2, The control gains of the two actuators at two ends of the frame are assumed to be the same. So, $n$ is 2, 2 and 4 in the case (1), case (2) and case (3) respectively. The multi-objective optimal design problem is stated as

$$\min\{\zeta_{\max}, \mathbf{K}_c^{\mathrm{T}}\mathbf{K}_c\}, \tag{16}$$

where, $\zeta_{\max}$ denotes the maximum ratio of the real part to the modulus of eigenvalues of the matrix $\mathbf{A}_{cl}$ defined in Equation (11), and it describes the stability margin of linear systems. The term $\mathbf{K}_c^{\mathrm{T}}\mathbf{K}_c$ denotes the *Frobenius* norm of the control gain matrix $\mathbf{K}_c$. Since the control system is optimised for zero initial conditions, the control effort cannot be included directly in the objective space and its *Frobenius* norm is used instead. By minimising this norm, the total control energy is also minimised.

To solve this MOOP, NSGA-II is used. Most of the default settings of this algorithm are kept and only two parameters are changed. They are population size and generation number. In this study, the population size is set to 500, and the number of generation is set to 1000. Also, in the optimisation process, we assume that the bogie moves at the speed of 350 km/h.

### 3.4. Multi-objective optimal control results

The Pareto front, Pareto set of multi-objective optimal in different control cases are discussed here. First of all, the optimal motor suspension parameters are investigated because the motor suspension parameters have an important influence on the bogie hunting stability. Moreover, the actuator outputs depend on the motor's states. For the optimisation of motor suspension parameters, we chose the minimum damping ratio that can be achieved by MOOP as an optimisation objective. The suspension frequency $f_{my}$ is used instead of

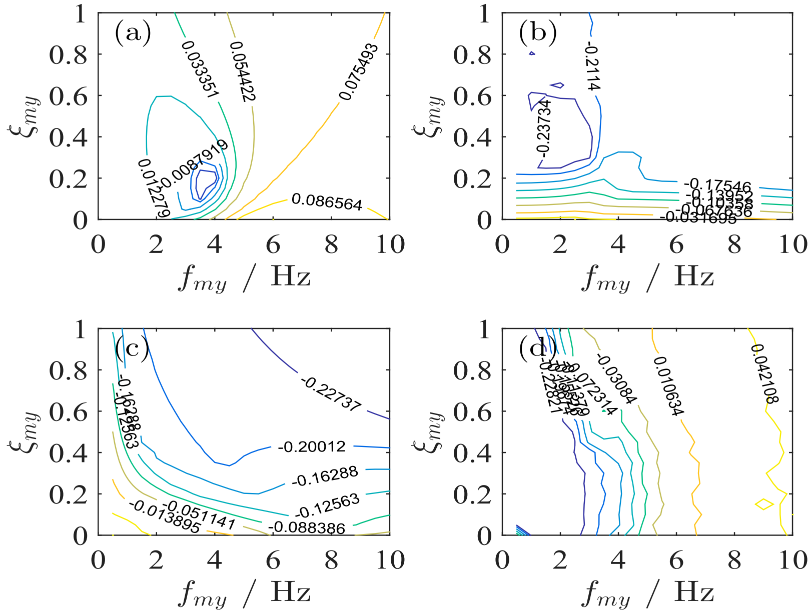


**Figure 2.** The motor suspension parameter optimisation in different cases. (a) Uncontrol; (b) Case (1); (c) Case (2); (d) Case (3).

the motor suspension stiffness to better understand the mechanism of motor flexible suspension [18,28]. The calculation range of motor suspension frequency $f_{my}$ is from 0 to 10 Hz and the range of motor suspension damping ratio $\xi_{my}$ (positive sign indicates a stable value) is 0 to 1. Figure 2 shows the maximum damping ratio $\zeta_{\max}$ of the bogie control system at different motor suspension parameters. Subgraph (a) shows that the optimal $f_{my}$ of 3 Hz and $\xi_{my}$ of 0.2 should be adopted in the bogie before applying active control. This parameters can be understand by the mechanism of dynamic vibration absorber caused by the flexible suspension motor [18]. To optimise the motor suspension parameters in different control cases, the minimum $\zeta_{\max}$ of the bogie control system at different motor suspension parameters was analysed with the optimal control gains calculated by MOOP. That is, the achievable minimum $\zeta_{\max}$ after applying control is the basis for selecting the motor suspension parameters. Subgraph (b) shows that the $f_{my}$ has little effect on the bogie hunting stability, but the influence of $\xi_{my}$ is obvious in case (1). Besides, the stability of the system is poor when the $\xi_{my}$ is small, and the $\zeta_{\max}$ tends to a constant value when the $\xi_{my}$ is larger than 0.3. In case (2), the larger the $f_{my}$ and $\xi_{my}$ are, the more stable the bogie is. In case (3), the optimal $f_{my}$ is from 3 to 5 Hz, and a larger $\xi_{my}$ is better for the system stability. According to the optimisation results of the three cases, the $f_{my}$ and $\xi_{my}$ are set to 3 Hz and 0.5 in every control case.

Figure 3 shows the Pareto front in different control cases. The Pareto front illustrates a conflicting relationship between $\zeta_{\max}$ and $\mathbf{K}_c^{\mathrm{T}}\mathbf{K}_c$. With the increase of control effort, the bogie is more stable. These results highlight the importance of the MOOP design. By having different design options, the decision-maker can choose any point from the solution set that meets the performance requirements. It can be seen from the figures that the linear system of bogie with fault of yaw damper is critical stability before applying the control at the

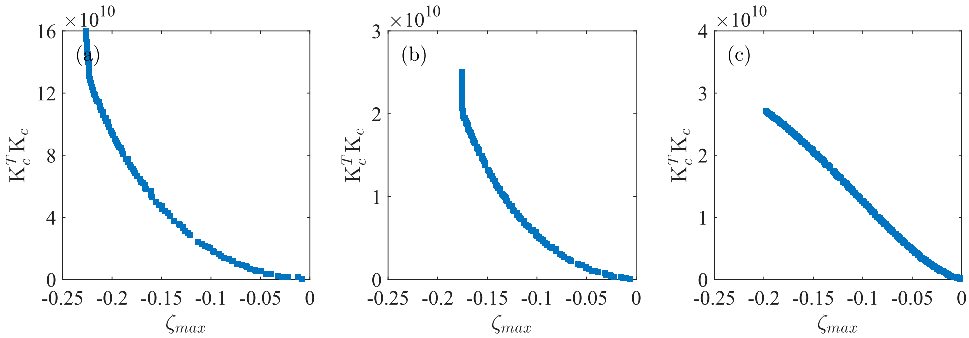


**Figure 3.** The Pareto front in different control cases. (a) Case (1); (b) Case (2); (c) Case (3).



speed of 350 km/h. The three control cases can effectively improve the system stability. The minimum $\zeta_{\max}$ can be achieved up to $-0.23$, $-0.18$, and $-0.2$, respectively, after applying active control. Figures 4 and 5 show the Pareto set of the three control cases, respectively. The corresponding displacement and velocity feedback gains of frame or motor need to be increased in order to meet the requirements of a better stability. In case (1), when the displacement and velocity feedback gains of frame, $k_p$ and $k_d$, are 1.2e4 and 1.2e5, the $\zeta_{\max}$ is $-0.15$. In case (2), the corresponding feedback gains of motor, $k_p$ and $k_d$, are $-8.6$e3 and 8.5e4 when the $\zeta_{\max}$ is $-0.15$. In case (3), the variation of frame's displacement feedback gain $k_{pf}$ and the motor's velocity feedback gain $k_{dm}$ have little effect on the bogie hunting stability. Meanwhile, the influences of the frame's velocity feedback gain $k_{df}$ and the motor's displacement feedback gain $k_{pm}$ on the system stability are obvious. Larger $k_{fd}$ and $k_{mp}$ are required with the increasing of system stability margin. The $\zeta_{\max}$ is $-0.15$ when the $k_{pf}$, $k_{df}$, $k_{pm}$ and $k_{dm}$ are $-660$, 7.7e4, 2.6e4, and $-15$, respectively. In this study, the $\zeta_{\text{set}}$ of $-0.15$ was set to get feedback gains from the Pareto sets of the three cases for the following analysis.

## 4. The linear stability analysis

### 4.1. Root locus analysis

The root locus of bogie linear system under frame lateral vibration control are analysed to verify the effectiveness of active control in the entire speed range. In every control case, the feedback gains are calculated based on the preset $\zeta_{\text{set}}$ of $-0.15$. Figures 6 and 7 show the root locus of bogie linear system in different control cases. Each root locus is composed of 25 sets of characteristic roots in speed range of 20–500 km/h, and each '+' indicates a corresponding mode. The larger symbol represents a larger running speed. The horizontal axis indicates the mode damping ratio $\zeta$ (negative sign indicates a stable value), which is the ratio of the real part to the modulus of eigenvalues of the matrix $\mathbf{A}_{cl}$ defined in Equation (11). The vertical axis indicates the damped vibration frequency of mode, which is the imaginary part of eigenvalues. Normally, as the speed increases, the hunting-related mode damping reduces. When the $\zeta$ is greater than 0, the hunting movement is unstable. Mostly, the low-frequency hunting mode determines the bogie hunting critical speed.

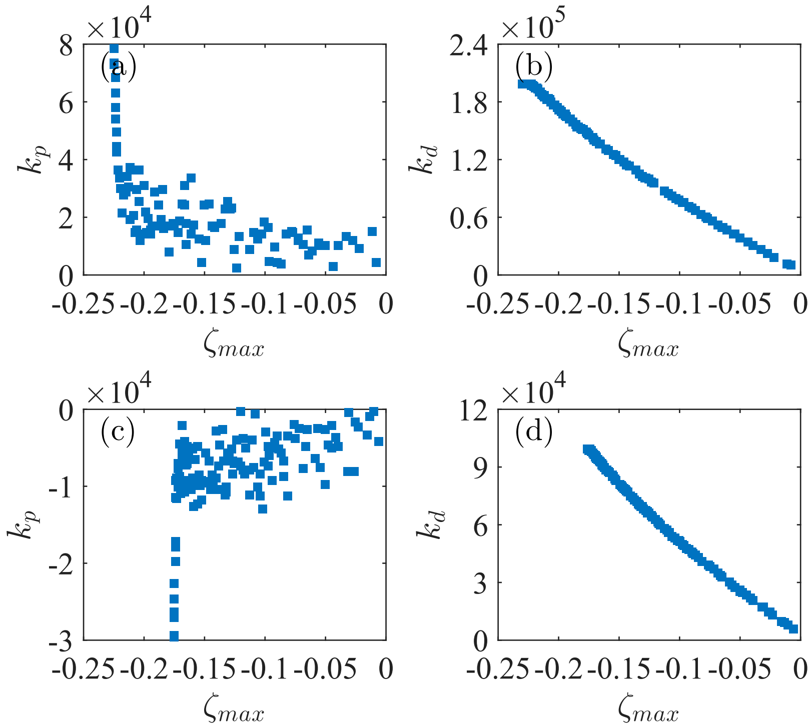


**Figure 4.** The Pareto set in control cases (1) & (2). (a)$k_p$ of case (1); (b)$k_d$ of case (1); (c)$k_p$ of case (2); (c)$k_d$ of case (2).

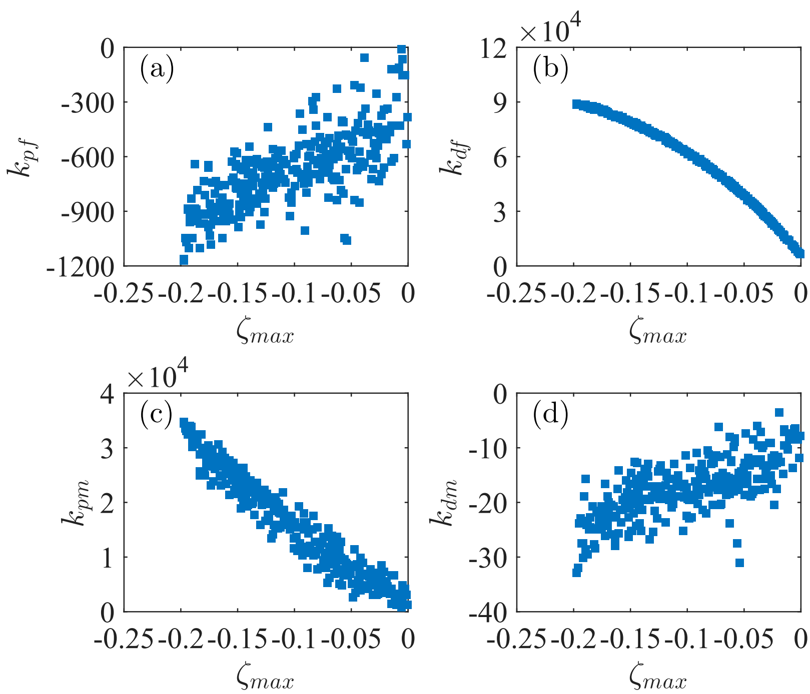


**Figure 5.** The Pareto set in control case (3).

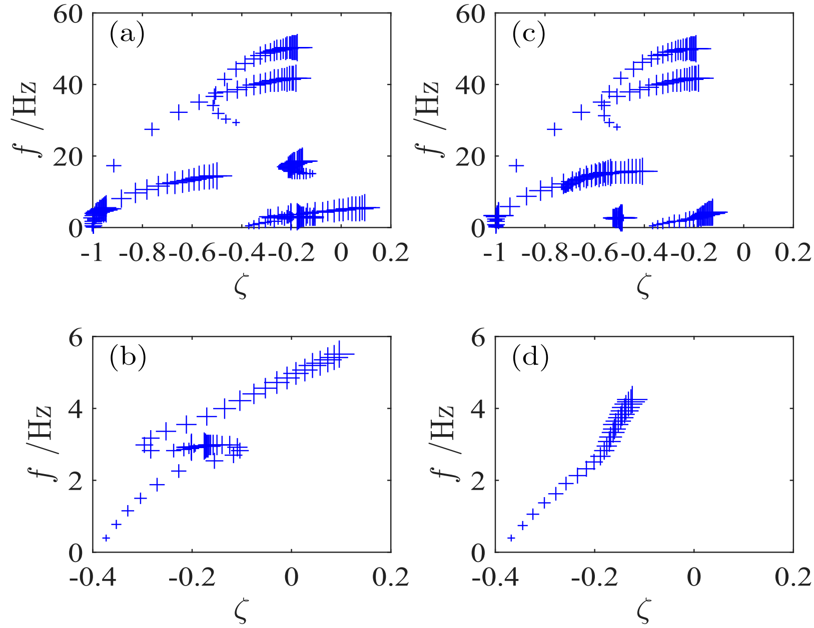


**Figure 6.** Bogie root locus in different control cases. (a) Uncontrol; (b) partial enlarged view of (a); (c) Case (1); (d) partial enlarged view of (c).

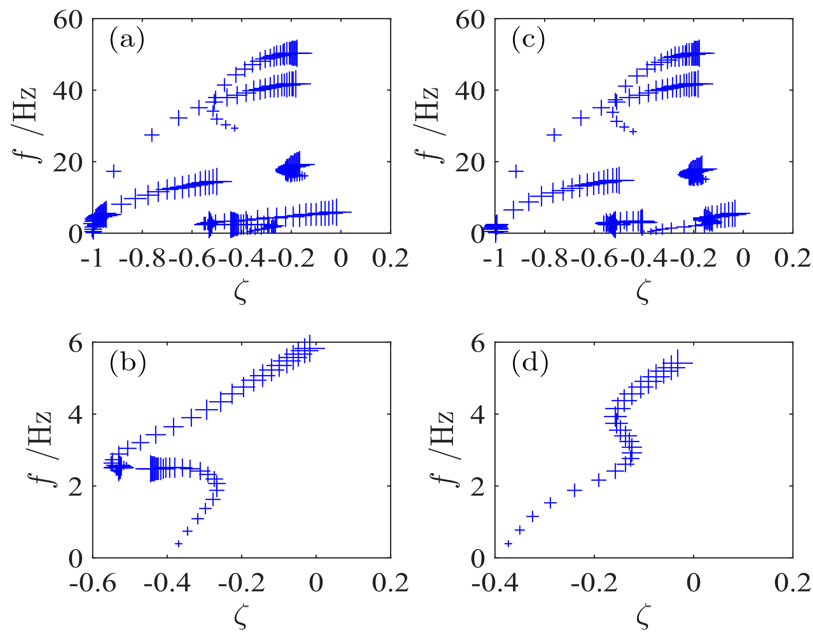


**Figure 7.** Bogie root locus in different control cases. (a) Case (2); (b) partial enlarged view of (a); (c) Case (3); (d) partial enlarged view of (c).

In Figure 6, Subgraph (a) shows the root locus before applying control. The linear critical speed of bogie with a fault of $c_{sx}$ is 350 km/h. Subgraph (b) shows a partial enlarged view of low- frequency bogie hunting mode. Due to the dynamic vibration absorbing function of the flexible suspension motor, the root locus of the bogie hunting mode is a S-like curve. The $\zeta$ reduces in a certain speed range, in which the bogie hunting frequency is close to the motor suspension frequency $f_{my}$. Subgraph (c) is the root locus of the system with control case (1), in which the actuators act on the frame transversely based on the feedback of frame states, and Subgraph (d) is a partial enlarged view of low-frequency bogie hunting mode. It is clear that the hunting stability improves sharply under the vibration control. The $\zeta_{\max}$ of the system is close to the preset value $\zeta_{\text{set}}$ of $-0.15$ no matter how fast the speed is.

Figure 7 shows the system root locus in cases (2) and (3), and corresponding partial enlarged views of the bogie low- frequency hunting mode. The bogie hunting stability improves in the two cases and the corresponding linear critical speeds are more than 500 km/h. Meanwhile, the shapes of the bogie hunting root locus curves in the three cases are significantly different. In case (1), as the speed increases, the bogie hunting damping ratio is close to $\zeta_{\text{set}}$ at high speeds. In case (2), the bogie hunting motion is more stable than the system with the control case (3) especially in low-to mid-speed range. That the feedback of motor's state in case (2) and the motor active flexible suspension in case (3) to suppress the frame lateral vibration are equivalent to improve the effects of motor vibration absorption. However, once the bogie hunting stability is enough, the $\zeta_{\max}$ of bogie control system is dependent on the frame lateral vibration mode, of which the vibration frequency is about 20 Hz. This is the reason why the system stability cannot be increased infinitely with the increasing of control effort, as shown in Figure 3.

### 4.2. The system parameter robustness analysis

In order to compare the robustness of the three types of control system against the perturbation of bogie dynamics parameters, the influence of bogie dynamic parameters on the system stability in different control cases is analysed. In this study, the feedback gains are obtained from the Pareto set according to the $\zeta_{\text{set}}$ of $-0.15$. A non-fault bogie model before applying control was used to compare the system stability after applying control. Figure 8 shows the calculated maximum system damping ratio $\zeta_{\max}$ of the bogie control system. In each subgraph, the horizontal axis is a varied dynamics parameter within a certain range, and the vertical axis is the $\zeta_{\max}$ of system with three control cases and a uncontrol case.

Subgraph (a) reflects the influence of running speed $v$ on the system stability. In the uncontrol case and case (1), as the speed increases, the value of $\zeta_{\max}$ increases and the system stability decreases. In case (2), the stability is the best at the speeds from 200 to 300 km/h, and then, the stability decreases significantly with the increasing of $v$. In case (3), the system stability is poor at the speed about 200 km/h, and it is the best at the speed of 350 km/h. In the three control cases, the stability decreases with the increasing of running speed if the speed is larger than 320 km/h. It indicates that we need to choose a higher speed as a calculation condition to optimise the control gains. In case (3), the bogie hunting stability needs to be checked in the low speed range.

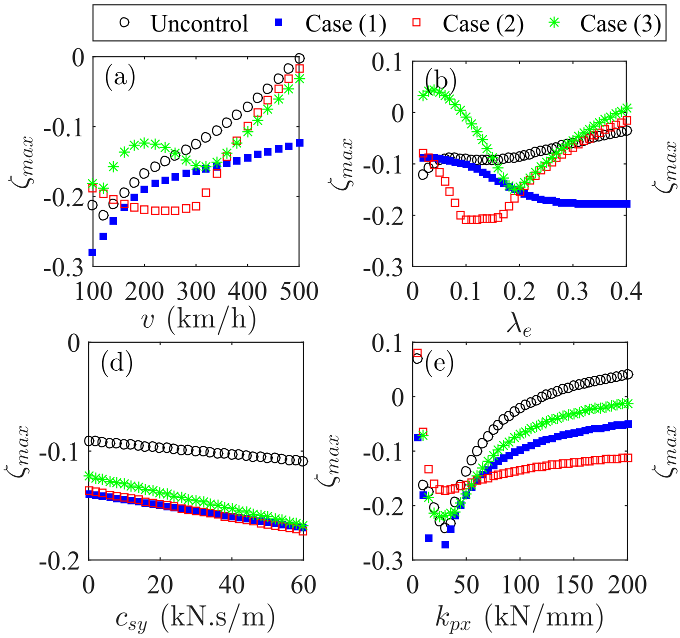


**Figure 8.** The linear system stability index with different dynamics parameters. (a) Speed $v$; (b) equivalent conicity $\lambda_e$; (c) yaw damper damping $c_{sx}$; (d) secondary lateral damper damping $c_{sy}$; (e) primary longitudinal stiffness $k_{px}$; (f) primary lateral stiffness $k_{py}$.

Subgraph (b) shows the influence of wheel/rail equivalent conicities $\lambda_e$ on the system stability. In case (1), the stability is the worst when $\lambda_e$ is 0.1. As the wheel/rail wear intensifies, $\lambda_e$ increases and the system stability changes better. In case (2) and (3), the stability is the best at $\lambda_e$ of 0.1–0.2 and 0.2, respectively, and then, the system stability becomes worse with the increasing of $\lambda_e$. In case (3), the stability deteriorates significantly when $\lambda_e$ is smaller than 0.15. Comparing to the other two control cases, the system stability of case (2) is the best in a new wheel/rail contact state, in which the $\lambda_e$ is about 0.1–0.2.

Subgraph (c) shows the influence of yaw damper damping $c_{sx}$ on the system stability. The stability improves with the increase of $c_{sx}$ except for case (3). Subgraph (d) shows the influence of second lateral damper damping $c_{sy}$. The impact of changed $c_{sy}$ on $\zeta_{\max}$ is not obvious, and the system stability improves slightly with the increase of $c_{sy}$. Subgraph (e) shows the influence of wheelset longitudinal stiffness $k_{px}$ on the system stability. In all case, the best $k_{px}$ is 30 kN/mm, and the stability of case (1) is the strongest at this value. Subgraph (f) demonstrates the influence of wheelset lateral stiffness $k_{py}$. In case (1) and (3), the optimal $k_{py}$ is 5 kN/mm, but in case (2), a larger $k_{py}$ is better.

In short, the frame lateral active vibration control can improve the robustness of bogie hunting stability against the perturbation of system dynamics parameters, such as $v$, $\lambda_e$ and $c_{sx}$, etc. The three control cases have different stability influence rules with the changing of system parameters. The robustness of control case (1) against the parameter perturbation is the strongest. However, the case (2) is more suitable for the dynamics performance requirements of vehicle.

## 5. The time-delay stability analysis

In a feedback control system, the time-delay caused by detecting and processing as well as response delay of actuator is inevitable. It is obvious that the effect of time-delay on the system dynamic performance. In this section, the influence of time-delay in the control system on bogie hunting stability is analysed using the continuous time approximation (CTA) method.

### 5.1. The CTA method

For the state Equation (1), it can be written as follows when the time-delay in feedback control is considered.

$$\begin{aligned} \dot{\mathbf{x}}(t) &= \mathbf{A}\mathbf{x}(t) + \mathbf{B}\mathbf{u}(t-\tau) + \mathbf{F}\mathbf{d}(t), \\ \mathbf{y} &= \mathbf{D}\mathbf{x}(t-\tau), \end{aligned} \tag{17}$$

where, $\tau$ is the time-delay of control system. Note that the system lives in a state space with an infinite dimension and the state vector is given by $(\mathbf{x}(t), \mathbf{x}(t-s),\ 0 < s \le \tau)$. Applying the CTA method [29–31], we discretise the delayed part of the state vector by considering a mesh $\Omega = \{\tau_i,\ i = 0, 1, \ldots, N\}$ of $N+1$ points in $[0, \tau]$ such that $0 = \tau_0 < \tau_1 < \cdots < \tau_{N-1} < \tau_N = \tau$. We define an extended state vector

$$\begin{aligned} \mathbf{X}(t) &= [\mathbf{x}(t), \mathbf{x}(t-\tau_1), \ldots, \mathbf{x}(t-\tau_N)]^{\mathrm{T}} \\ &= [\mathbf{x}_1(t), \mathbf{x}_2(t), \ldots, \mathbf{x}_{N+1}(t)]^{\mathrm{T}}. \end{aligned} \tag{18}$$

After introducing an interpolation scheme of $\mathbf{x}(t-\tau_i)$ over the mesh grid $\tau_i$, we obtain an equation for the vector $\mathbf{X}(t)$ without an explicit time-delay to replace Equation (1).

$$\begin{aligned} \dot{\mathbf{X}}(t) &= \bar{\mathbf{A}}\mathbf{X}(t) + \bar{\mathbf{F}}\mathbf{d}(t) \\ \mathbf{Y} &= \bar{\mathbf{D}}x(t-\tau), \end{aligned} \tag{19}$$

where, $\bar{\mathbf{A}}$, $\bar{\mathbf{F}}$, $\bar{\mathbf{D}}$ are extended matrix. $\bar{\mathbf{A}}$ is given by

$$\bar{\mathbf{A}} = \begin{bmatrix} \mathbf{A} & & \cdots & \mathbf{B} \\ \dfrac{\mathbf{I}}{\Delta\tau} & -\dfrac{\mathbf{I}}{\Delta\tau} & & \\ \vdots & & \ddots & \vdots \\ & \cdots & \dfrac{\mathbf{I}}{\Delta\tau} & -\dfrac{\mathbf{I}}{\Delta\tau} \end{bmatrix}, \tag{20}$$

where, $\Delta\tau = \tau/N$, $\mathbf{I}$ is identity matrix and has the same dimension with $\mathbf{A}$. The stability analysis of time-delay system can be carried out by calculating the eigenvalues of $\bar{\mathbf{A}}$.

### 5.2. The stability of time-delay system

We can analyse the stability of linear time-delay system by the CTA method. In this study, the delayed part of the state vector is extended to 20 points, and the feedback gains in three cases are also selected based on the $\zeta_{\text{set}}$ of $-0.15$ from the multi-objective optimisation

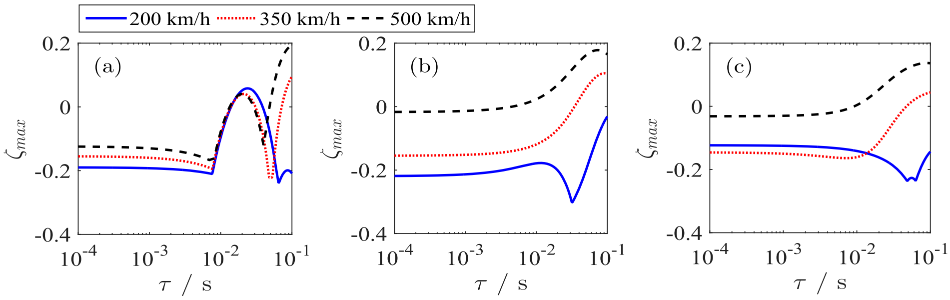


**Figure 9.** The effect of time-delay on the system stability at different speeds. (a) Case (1); (b) Case (2); (c) Case (3).



results in Section 3.4. Figure 9 shows the maximum damping ratio $\zeta_{\max}$ versus time-delay at three different running speeds of 200, 350, and 500 km/h, respectively. Subgraph (a) is the results of case (1). The calculation results at the three speeds are basically consistent. When the delay $\tau$ is less than 7 ms, it slightly improves the system stability, and the $\zeta_{\max}$ at the speed of 350 km/h reduces from $-0.15$ to $-0.19$ with the delay of 7 ms. When the delay is larger than 7 ms, the $\zeta_{\max}$ suddenly increases to 0.04 and the system becomes unstable. In case (2), the system stability decreases with the increase of delay at high speeds. The stability decreases obviously when the delay is larger than 10 ms. However, the system stability improves when the delay is about 30 ms at speed of 200 km/h. In case (3), the influence of the time-delay is basically consistent with the case (2). The delay decreases the system stability at high speeds. At the speed of 200 km/h, the increasing time-delay within a certain range is favourable to the system stability. An appropriate time-delay can be used to improve the system stability.

In order to understand the influence of time-delay on the system stability, the root locus of the bogie control system considering the time-delay is analysed. Figure 10 shows the root locus of the system including delay in feedback control. The CTA method is used to extend the dimension of the original system matrix. Compared to the system without delay, the time-delay system has more vibration modes with large damping, but the large damping does not affect the system dynamic performances. Additionally, the time-delay affects the damping ratio of low-frequency hunting mode, thus affecting the system stability. In case (1), as shown in Figure 10 (a) and (b), the delay improves the stability of low-frequency hunting mode, of which the frequency is smaller than 6 Hz. However, the delay causes a speed independent unstable mode, which is the frame lateral vibration mode and its frequency is about 20 Hz. It results in a sharp increase of $\zeta_{\max}$, even the control system instability, as shown in Figure 9(a). In case (2) and (3), the delay makes the root locus curves of low-frequency hunting mode in low speed range shift to the left. Meanwhile, it also makes the root locus curves of low-frequency hunting modes at high speeds shift to the right. So, the time-delay affects the system stability differently in different speed ranges. It can be understood that the time-delay reduces the system stability, but it also enhances the function of active dynamic vibration absorber caused by the lateral flexible suspension motor. So, the stability improves in a certain speed range, in which the bogie hunting frequency is close to the motor suspension frequency.

In summary, when the frame vibration is controlled by two inertial actuators based on the feedback states of frame directly, as shown in case (1), the bogie hunting is stable

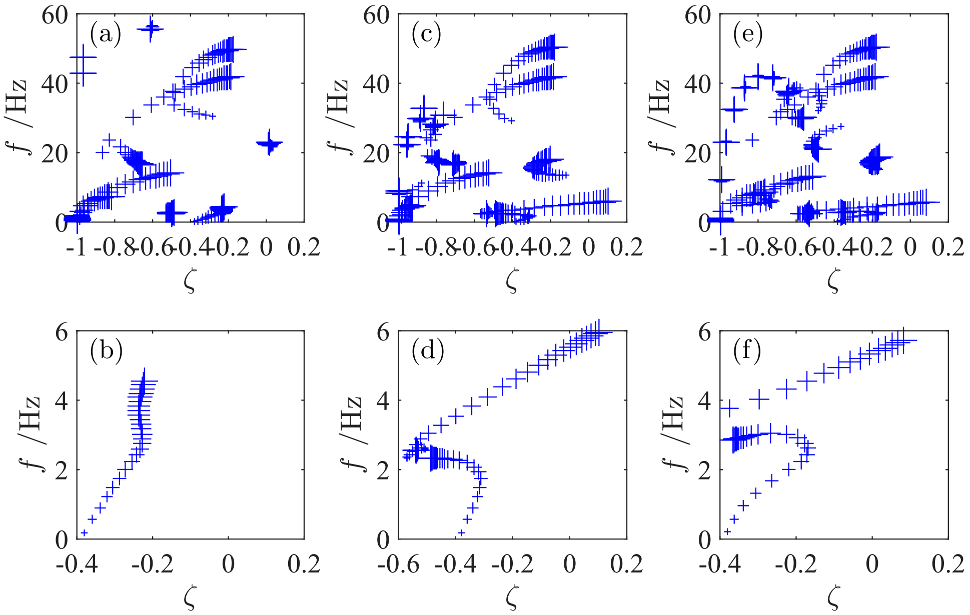


**Figure 10.** The root locus of the bogie control system with delay. (a) Case (1) with delay of 15 ms; (b) partial enlarged view of (a); (c) Case (2) with delay of 30 ms; (d) partial enlarged view of (c); (e) Case (3) with delay of 30 ms; (f) partial enlarged view of (e).

no matter how fast the speed is, but the time-delay within a certain range may lead to control instability, thus deteriorating the bogie dynamic performances. In case (2) and (3), the frame vibration is controlled based on the feedback states including the motor's states. Although delay is not conducive to the system stability, it makes the active dynamic vibration absorbing caused by the lateral flexible suspension motor more effective, thus improving the bogie hunting stability in a certain speed range. More than delay in control system, the dynamics of the actuation and sensing should be considered in future works.

## 6. The nonlinear stability analysis

The railway vehicle is a typical nonlinear dynamic system, which is mainly reflected in the nonlinear characteristics of the wheel–rail contact relationship and the suspension elements. The nonlinearity of wheel–rail contact includes the wheel–rail contact geometry and the saturation of wheel–rail creep force. The nonlinear critical speed is an important index for railway vehicles. The actual vehicle nonlinear critical speed depends on the external excitation. It is very important to analyse the nonlinear bifurcation behaviour for understanding the vehicle lateral dynamic performances. In this section, a nonlinear bogie lateral dynamics model was established and the nonlinear bifurcation of wheelset lateral displacement versus running speed under the frame vibration control was analysed by a direct integral method.

The nonlinear characteristics of wheel–rail contact geometry and creep saturation are taken into account in the bogie nonlinear dynamics model. Based on the previous linear dynamics model, the wheel–rail contact equivalent conicity $\lambda_e'$ can be expressed by a

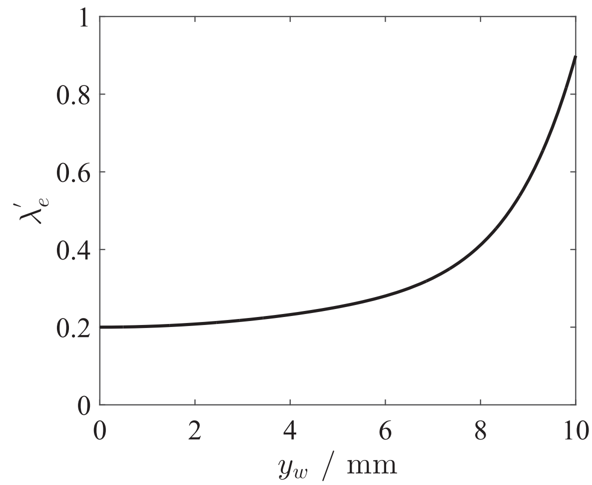


**Figure 11.** The nonlinear wheel–rail contact equivalent conicity.

polynomial which is a nonlinear function about the wheelset lateral displacement $y_w$, as follows:

$$\lambda_e' = a_0 + a_1 y_w^2 + a_2 y_w^6 + a_3 y_w^8. \tag{21}$$

where, for a new wheel–rail contact, $a_0 = \lambda_e$, $a_1 = 2.0\text{e}3$, $a_2 = -1.0\text{e}9$, $a_3 = 5.0\text{e}15$. The $\lambda_e'$ at different wheelset lateral displacement is shown in Figure 11. Shen's method [32] was adopted to calculate the wheel–rail nonlinear creep force. In order to highlight the effect of active control on improving the bogie hunting stability, the fault of yaw damper was conducted.

According to the results of linear stability analysis, the case (1) has a strong robustness, no matter how fast the bogie running speed is, the maximum damping ratio $\zeta_{\max}$ of the bogie system is always close to the preset $\zeta_{\text{set}}$. Therefore, the nonlinear bifurcation does not exist in case (1). In this case, the delay over 10 ms will lead to instability of control system, which is verified by the time domain integral of the nonlinear model. Figure 12 shows the wheelset lateral displacement curves of the bogie nonlinear model at a speed of 350 km/h.

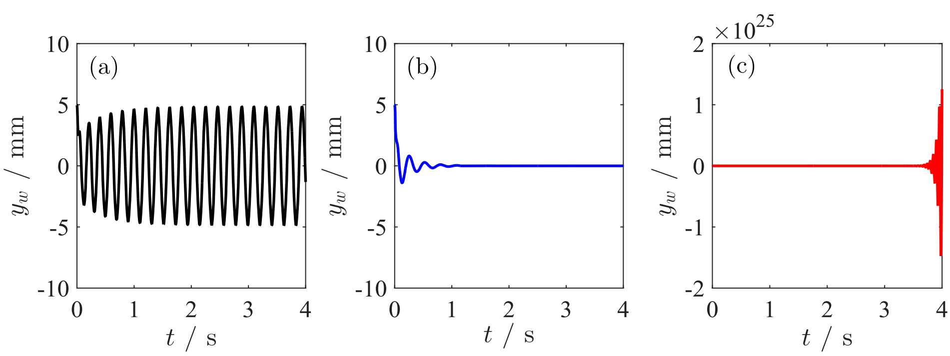


**Figure 12.** The wheelset lateral displacement in time domain. (a) Uncontrol; (b) Case (1) without delay; (c) Case (1) with delay of 15 ms.

Subgraph (a) is the results before applying active control, in which the bogie hunting is unstable. Subgraph (b) and (c) show the results when the delay in case (1) is 0 and 15 ms, respectively. It is concluded that the delay of 15 ms makes the control system unstable.

The bogie hunting bifurcation can be obtained using the direct integration of the nonlinear model with a changed initial value, which is an approximate periodic solution and was calculated by numerical integration. Figure 13 shows the bifurcation curves of wheelset lateral displacement versus running speed in different calculation condition. The blue points in the figure represent the stable limit cycles, and the red points represent the unstable limit cycles. For the new wheel–rail contact, the bogie hunting has a typical subcritical bifurcation in all cases. The corresponding speed of a point where the vertical coordinate equals 0 is called the linear critical speed, and the minimum speed of the unstable limit cycle is the nonlinear critical speed. The critical speeds of the bogie in different states are shown in Table 2.

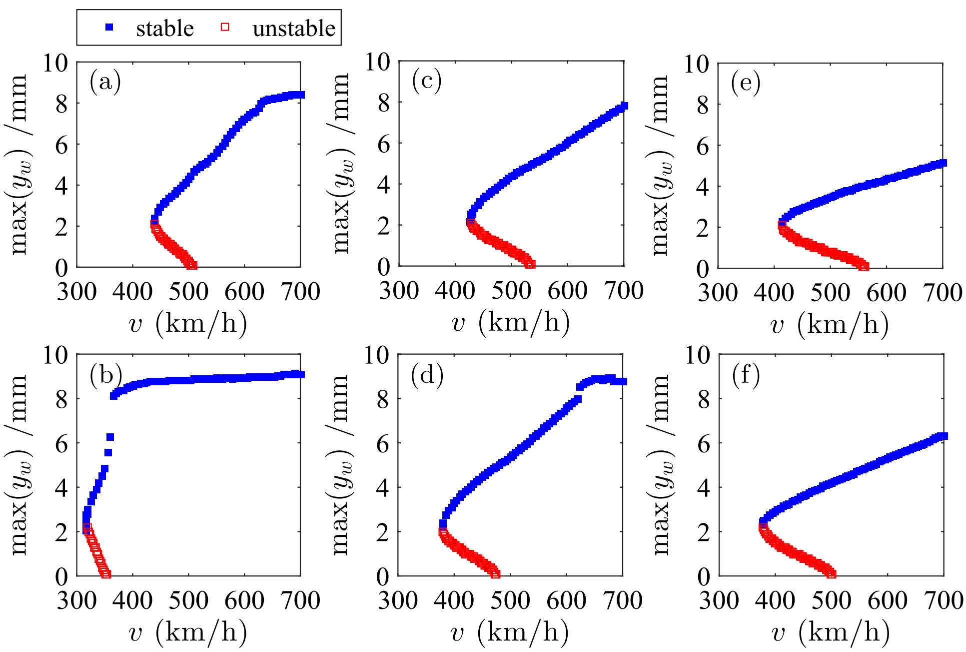


**Figure 13.** The wheelset lateral displacement bifurcation curves about the running speed in different control conditions. (a) Uncontrol without fault; (b) uncontrol with fault of $c_{sx}$; (c) Case (2) without delay; (d) Case (2) with delay of 10 ms; (e) Case (3) without time-delay; (f) Case (3) with delay of 10 s.

**Table 2.** The calculated linear and nonlinear critical speeds.

| | Critical speed (km/h) | | |
|---|---|---|---|
| Item | Linear | Nonlinear | Remark |
| (a) | 509 | 439 | No fault; uncontrol. |
| (b) | 353 | 319 | Fault; uncontrol. |
| (c) | 536 | 428 | Fault; Case(2) without delay. |
| (d) | 474 | 380 | Fault; Case(2) with delay of 10 ms. |
| (e) | 561 | 415 | Fault; Case(3) without delay. |
| (f) | 501 | 377 | Fault; Case(3) with delay of 10 ms. |

With the fault of $c_{sx}$, the bogie nonlinear critical speed cannot meet the requirement of running at the speed of 350 km/h. In case (2) and (3), the bogie linear and nonlinear critical speeds are larger than 500 and 400 km/h respectively, which are equivalent to the stability of the uncontrolled bogie without fault of $c_{sx}$. When a delay of 10 ms is considered, the linear and nonlinear critical speeds are reduced by about 60 and 40 km/h, respectively.

## 7. Conclusions

(1) In this study, three cases of control configurations about frame lateral vibration control were proposed to improve the hunting stability of a high-speed train bogie. For case (1) and (2), in which two inertial actuators act on the front and rear end beam of frame, the control takes only four measurements of motion of bogie frame or motor respectively. For case (3), in which a retractable actuator acts between frame and motor, there are eight measurements of motion, that is, the lateral displacement and yaw angle and their first derivatives of frame, as well as the lateral displacements of two motors and their first derivatives. A partial state feedback control applied to the underactuated and unobservable bogie system, and the multi-objective optimisation with two objective functions about the stability index and the control effort was solved by the NSGA-II algorithm for getting the feedback gains.

(2) The linear stability of the bogie control system including a fault of yaw damper and time-delay in control system was analysed. For the three control cases, the motor suspension parameters were optimised with an object of stability index. The analysis results show that the three control cases could stabilise the bogie hunting movement effectively. Meanwhile, the root locus of bogie low-frequency hunting mode which determinates the system critical speed is different. Therefore, the different control case shows a different dynamics performances with the increasing of speed. In additional, the system stability and control robustness against the perturbation of bogie dynamics parameters were compared. The results show that the robustness of the case (1) is the strongest. However, the case (2) is more suitable for the dynamic performance requirements of vehicle.

(3) The effect of time-delay in control system on the bogie hunting stability was analysed by a linear analysis method. In the three cases, the delay over 10 ms is harmful to the stability of the bogie control system obviously. For case (1), the delay within 10–40 ms will lead to control instability, in which the damping ratio of frame lateral vibration mode is larger than 0. For case (2) and (3), at some speeds, such as 200 km/h, the increasing delay within a certain range is favourable to the bogie hunting stability. That is because the delay enhances the function of active dynamic vibration absorber caused by the lateral flexible suspension motor. At last, the nonlinear stability and time domain results of the bogie control system were analysed by the numerical integration method to verify the linear analysis.

## Acknowledgements

In addition, the first author would like to thank the China Scholarship Council (CSC) for sponsoring his study in USA.

## Disclosure statement

No potential conflict of interest was reported by the authors.


## Funding

The material in this paper is based on work supported by grants (51675443, 11172197, 11332008 and 11572215) from the National Natural Science Foundation of China, and a Key Laboratory grant (Nos. 2015TPL_T10, 2017TPL_T02) of the Independent Research and Development Projects.


## References


[1] Goodall RM, Kortüm W. Mechatronic developments for railway vehicles of the future. Control Eng Pract. 2002;10(8):887–898.

[2] Ward CP, Weston PF, Stewart EJC, et al. Condition monitoring opportunities using vehicle-based sensors. Proc Inst Mech Eng Part F: J Rail Rapid Transit. 2011;225(2):202–218.

[3] Pearson JT, Goodall RM, Mei TX, et al. Active stability control strategies for a high speed bogie. Control Eng Pract. 2004;12(11):1381–1391.

[4] Abood KHA, Khan RA. Investigation to improve hunting stability of railway carriage using semi-active longitudinal primary stiffness suspension. J Mech Eng Res. 2010;2(5):97–105.

[5] Pearson JT, Goodall RM, Mei TX, et al. Design and experimental implementation of an active stability system for a high speed bogie. Vehicle Syst Dyn. 2004;41:43–52.

[6] Gretzschel M, Jaschinski A. Design of an active wheelset on a scaled roller rig. Vehicle Syst Dyn. 2004;41(5):365–381.

[7] Wickens AH. Comparative stability of bogie vehicles with passive and active guidance as influenced by friction and traction. Vehicle Syst Dyn. 2009;47(9):1137–1146.

[8] Mei TX, Goodall RM. Recent development in active steering of railway vehicles. Vehicle Syst Dyn. 2003;39(6):415–436.

[9] Perez J, Busturia JM, Goodall RM. Control strategies for active steering of bogie-based railway vehicles. Control Eng Pract. 2002;10(9):1005–1012.

[10] Wei X, Zhu M, Jia L. A semi-active control suspension system for railway vehicles with magnetorheological fluid dampers. Vehicle Syst Dyn. 2016;54(7):982–1003. Available from: http://dx.doi.org/10.1080/00423114.2016.1177189.

[11] Ahmadian M, Mohan A. Semiactive control of hunting stability in rail vehicles. In: Proceeding of ASME international mechanical engineering congress and exposition (IMECE'05). 2005 Nov ; Orlando, FL, USA; p. 63–68.

[12] Bruni S, Goodall R, Mei TX, et al. Control and monitoring for railway vehicle dynamics. Vehicle Syst Dyn. 2007;45(7–8):743–779.

[13] Alonso A, Giménez JG, Gomez E. Yaw damper modelling and its influence on railway dynamic stability. Vehicle Syst Dyn. 2011;49(9):1367–1387.

[14] Zhai W, Liu P, Lin J, et al. Experimental investigation on vibration behaviour of a CRH train at speed of 350 km/h. Int J Rail Transport. 2015;3(1):1–16. Available from: http://dx.doi.org/10.1080/23248378.2014.992819.

[15] Goodall RM, Bruni S, Mei TX. Concepts and prospects for actively controlled railway running gear. Vehicle Syst Dyn. 2006;44(suppl. 1):60–70. Available from: http://dx.doi.org/10.1080/00423110600867374.

[16] Mei TX, Goodall RM. Stability control of railway bogies using absolute stiffness: sky-hook spring approach. Veh Syst Dyn. 2006;44(suppl. 1):83–92. Available from: http://dx.doi.org/10.1080/00423110600867440.

[17] Zolotas AC, Pearson JT, Goodall RM. Modelling requirements for the design of active stability control strategies for a high speed bogie. Multibody Syst Dyn. 2006;15(1):51–66. Available from: http://dx.doi.org/10.1007/s11044-006-2361-5.

[18] Yao Y, Zhang H-J, Luo S-H. The mechanism of drive system flexible suspension and its application in locomotives. Transport. 2015;30(1):69–79.

[19] Pareto V. Manual of political economy. London: The MacMillan Press; 1971 (original edition in French in 1927).
[20] Hernández C, Naranjani Y, Sardahi Y, et al. Simple cell mapping method for multi-objective optimal feedback control design. Int J Dyn Control. 2013;1(3):231–238.
[21] Jones DF, Mirrazavi SK, Tamiz M. An Multi-objective meta-heuristics: an overview of the current state-of-the-art. Eur J Oper Res. 2002;137(1):1–9.
[22] Marler RT, Arora JS. Survey of multi-objective optimization methods for engineering. Struct Multidiscip Optim. 2004;26(6):369–395.
[23] Srinivas N, Deb K. Muiltiobjective optimization using nondominated sorting in genetic algorithms. Evol Comput. 1994;2(3):221–248.
[24] Deb K, Pratap A, Agarwal S, et al. A fast and elitist multiobjective genetic algorithm: Nsga-ii. IEEE Trans Evol Comput. 2002;6(2):182–197.
[25] Beyer H-G, Deb K. On self-adaptive features in real-parameter evolutionary algorithms. IEEE Trans Evol Comput. 2001;5(3):250–270.
[26] Deb K, Agrawal RB. Simulated binary crossover for continuous search space. Complex Syst. 1995;9(2):115–148.
[27] Raghuwanshi MM, Kakde OG. Survey on multiobjective evolutionary and real coded genetic algorithms. In: Proceedings of the 8th Asia Pacific symposium on intelligent and evolutionary systems; Cairns, Australia; 2004. p. 150–161.
[28] Yao Y, Zhang X, Liu X. The active control of the lateral movement of a motor suspended under a high-speed locomotive. Proc Inst Mech Eng Part F: J Rail Rapid Transit. 2015. Available from: doi.org/10.1177/0954409715605138.
[29] Sun J-Q. A method of continuous time approximation of delayed dynamical systems. Commun Nonlinear Sci Numer Simul. 2008;14(4):998–1007.
[30] Sun J-Q. Finite dimensional Markov process approximation for stochastic time-delayed dynamical systems. Commun Nonlinear Sci Numer Simul. 2009;14(5):1822–1829.
[31] Huan R-H, Chen L-X, Sun J-Q. Multi-objective optimal design of active vibration absorber with delayed feedback. J Sound Vib. 2015;339:56–64.
[32] Shen ZY, Hedrick JK, Elkins JA. A comparison of alternative creep force models for railvehicle dynamic analysis. In: Proceeding of 8th IAVSD symposium on vehicle system dynamics, dynamics of vehicles on roads and tracks. MIT, Cambridge: Swets and Zeitlinger; 1984. p. 591–605.

## Appendix

The matrices of the bogie system in Equation (1) are listed below.

$$\mathbf{M}=\begin{bmatrix} m_w &&&&&&& \\ & I_w &&&&&& \\ && m_w &&&&& \\ &&& I_w &&&& \\ &&&& m_f &&& \\ &&&&& I_f && \\ &&&&&& m_m & \\ &&&&&&& m_m \end{bmatrix}$$

$$\mathbf{K}=\begin{bmatrix} k_{py}+k_{gy} & -2f_\eta & & & -k_{py} & -bk_{py} & & \\ \dfrac{2\lambda_e l_0 f_\zeta}{r_0} & l_1^2k_{px}+k_{g\psi} & & & & -l_1^2k_{px} & & \\ & & k_{py}+k_{gy} & -2f_\eta & -k_{py} & bk_{py} & & \\ & & \dfrac{2\lambda_e l_0 f_\zeta}{r_0} & l_1^2k_{px}+k_{g\psi} & & -l_1^2k_{px} & & \\ -k_{py} & & -k_{py} & & 2k_{py}+k_{sy}+2k_y & & -k_{my} & -k_{my} \\ -bk_{py} & -l_1^2k_{px} & bk_{py} & -l_1^2k_{px} & & \begin{matrix} l_2^2k_{sx}+2l_1^2k_{px} \\ +2b^2k_{py}+2l_m^2k_{my} \end{matrix} & -l_mk_{my} & l_mk_{my} \\ & & & & -k_{my} & -l_mk_{my} & k_{my} & \\ & & & & -km_y & l_mk_{my} & & k_{my} \end{bmatrix}$$

$$\mathbf{C}=\begin{bmatrix} \dfrac{2f\eta}{v} &&&&&&& \\ & \dfrac{2l_0^2f_\zeta}{v} &&&&&& \\ && \dfrac{2f\eta}{v} &&&&& \\ &&& \dfrac{2L_0^2f_\zeta}{v} &&&& \\ &&&& c_{sy}+2c_{my} && -c_{my} & -c_{my} \\ &&&&& l_2^2c_{sx}+l_m^2c_{my} & -l_mc_y & l_mc_{my} \\ &&&& -c_{my} & -l_mc_{my} & c_{my} & \\ &&&& -c_{my} & l_mc_{my} && c_{my} \end{bmatrix}$$

$$\text{Case (1)\&(2)}: \mathbf{E}=\begin{bmatrix} 0 & 0 & 0 & 0 & 1 & l_e & 0 & 0 \\ 0 & 0 & 0 & 0 & 1 & -l_e & 0 & 0 \end{bmatrix}^{\mathrm{T}}$$

$$\text{Case (3)}: \mathbf{E}=\begin{bmatrix} 0 & 0 & 0 & 0 & 1 & l_m & -1 & 0 \\ 0 & 0 & 0 & 0 & -1 & l_m & 1 & 0 \end{bmatrix}^{\mathrm{T}}.$$